orange crystalline **23**. Iodination of this species with 1.5 equiv of *N*-bromosuccinimide, which produced an immediate color change from orange to dark orange-brown, gave 127 mg (0.34 mmol, 99%) of orange crystalline **24**. The latter compound was also obtained quantitatively on treatment of **1** with 2.5 equiv of *N*-iodosuccinimide. Anal. Calcd for $CoIC_{16}B_3H_{29}$ (**23**): C, 43.71; H, 6.65. Found: C, 44.17; H, 6.61.

Synthesis of $(C_5Me_5)Co(2,3\text{-}Et_2C_2B_3H_4\text{-}5\text{-}CN)$ (25) and $(C_5Me_5)Co(2,3\text{-}Et_2C_2B_3H_4\text{-}4/6\text{-}CN)$ (26). *p*-Toluenesulfonyl cyanide (0.627 g, 3.46 mmol) was added via a tip-tube to a solution of 1^- (0.290 g, 0.92 mmol) at −78 °C, producing a brownish-yellow solution. The bath was removed and the solution stirred for 30 min, after which the solvent was removed and the residue was washed with CH_2Cl_2 and then column-chromatographed starting with hexane, which produced **1** (0.124 g, 43% recovery). The solvent was changed to 1:1 hexane/CH_2Cl_2, affording one band which was collected and placed on a TLC plate in the same solvent. Two bands were obtained, the first of which was **25** (35 mg, 0.10 mmol, 11%) and the second was **26** (23 mg, 0.07 mmol, 8%). Anal. Calcd for $CoNC_{17}B_3H_{29}$ (**25**): N, 4.13; C, 60.27; H, 8.63. Found: N, 4.09; C, 60.53; H, 8.62. Visible–UV absorptions: 288 (87%), 244 (27%), 234 (32%). Anal. Calcd for $CoNC_{17}B_3H_{29}$ (**26**): N, 4.13; C, 60.27; H, 8.63. Found: N, 3.92; C, 60.50; H, 8.60. Visible–UV absorptions: 286 (95%), 248 (50%), 234 (43%).

Synthesis of $(C_5Me_5)Co(2,3\text{-}Et_2C_2B_3H_4\text{-}4/6\text{-}NO_2)$ (27). Nitronium tetrafluoroborate (4.5 mL of 0.5 M solution in sulfolane, 2.25 mmol) was added to 1^- (0.301 g, 0.96 mmol) at −78 °C. The solution immediately turned brown. After stirring at −78 °C for 30 min and at room temperature for 30 min, the solvent was removed and the residue washed with hexane followed by CH_2Cl_2. The hexane wash was column-chromatographed in hexane, affording only **1** (0.048 g, 16% recovery). The CH_2Cl_2 wash was chromatographed on a silica column in 1:1 hexane/CH_2Cl_2, giving a band of **1** followed by a small band of **27** (5 mg, 0.01 mmol, 1.5%), identified by ^1H NMR and mass spectroscopy.

Reaction of 1^- with Vinyl Bromide. Vinyl bromide (1.03 mmol) was reacted with 1^- (0.303 g, 0.96 mmol) under the conditions of the preceding synthesis, affording on workup only **1** (55% recovery) and a trace of an air-sensitive compound whose ^1H NMR and mass spectra were consistent with the formulation as a vinyl derivative, $(C_5Me_5)Co(2,3\text{-}Et_2C_2B_3H_4CH{=}CH_2)$ (**28**).

Other Attempted Reactions of 1^-. Treatment of 1^- with excess methanesulfonyl fluoride gave only **1** (46% recovery). Reaction with excess *p*-toluenesulfonyl isocyanate resulted in the loss of all starting material and gave no characterizable product. Reactions of 1^- with 1 equiv of benzoyl chloride or malonyl chloride gave only **1** in ca. 50% recovery.

X-ray Structure Determination on 2. Relevant crystal data and experimental parameters are listed in Table VI. Intensities were collected on a Nicolet P3m diffractometer (Mo Kα, λ = 0.7107 Å). The unit cell was determined using the setting angles of 20 high-angle reflections. The intensities of three standard reflections were monitored showing no significant decay. Empirical absorption corrections were made using the program DIFABS[19] with transmission factors in the range 0.88–1.22. All calculations were performed on a VAXstation 3520 computer using the TEXSAN 5.0 crystallographic software package.[20] The structure was solved by heavy-atom techniques (Patterson and Fourier maps). Full-matrix least-squares refinement with anisotropic thermal parameters for all non-hydrogen atoms yielded the final *R* of 0.037. All hydrogen atoms were located from the difference Fourier maps and included as fixed contributions to the structure factors. Only those reflections for which $I > 3.0\sigma(I)$ were used in the final refinement of the structural parameters.

Acknowledgment. The support of the National Science Foundation (Grant No. CHE 90-22713) and the U.S. Army Research Office is gratefully acknowledged. We thank Professor Frank Carey for enlightening discussions on O-acylation mechanisms, Mark Benvenuto for the unit-resolution mass spectra, Dr. Xiangsheng Meng for the ^{11}B NMR spectra, and Markus Hölscher for the preparation of the B(4,5,6)-trichloro derivative. We are indebted to Dr. James Davis for initiating work on the reaction of 1^- with acetyl chloride.

OM920014G

(19) Walker, N.; Stuart, D. *Acta Crystallogr.* **1983**, *A39*, 158.
(20) *TEXSAN: Single Crystal Structure Analysis Software*, Version 5.0; Molecular Structure Corp.: The Woodlands, TX 77381, 1989.

Tungsten–Oxo Complexes with Amido Ligands: A Simple Example of the Stereochemical and Dynamic Consequences of Competing π-Donor Effects

Jean Pierre Le Ny, Marie-Thérèse Youinou, and John A. Osborn*

Laboratoire de Chimie des Métaux de Transition et de Catalyse (URA 424 du CNRS), 4 rue Blaise Pascal, 67000 Strasbourg, France

Received September 27, 1991

Complexes of tungsten(VI) of the type $WO(CH_2Bu^t)_2(NR_2)Cl$ **1** and $WO(CH_2Bu^t)_3(NR_2)$ **2** (**1a**, **2a**, R = Et; **1b**, **2b**, R = Me; **2c**, R = pyrrolidinate) have been synthesized and characterized. The proton NMR spectra of these compounds indicated that the stereochemistry was different from that of the chloride analogues. Further, the variable-temperature NMR data showed these complexes to be stereochemically nonrigid where exchange of the NR_2 group or equilibration of the neopentyl groups occurred. The structure of $WO(CH_2Bu^t)_3(NEt_2)$ (**2a**) was established by X-ray diffraction and is in agreement with the NMR observations; the amido ligand adopts a position cis to the oxo, with the NR_2 group parallel to the W=O vector. This ligand arrangement results from the competing π-donor demands of the amido and oxo ligands. $C_{19}H_{43}NOW$ crystallizes in the monoclinic space group $P2_1/c$ (No. 14), a = 9.632 (2) Å, b = 12.961 (3) Å, c = 18.192 (4) Å, β = 104.62 (2)°, V = 2197.6 Å^3, Z = 4, ρ(calcd) = 1.467 g cm^{-3}, R_F = 0.0276, R_{wF} = 0.0514.

Introduction

For several years we have been interested in high-oxidation-state organometallic chemistry, particularly that of W(VI) and Mo(VI). The role played by strong π-donor ligands (e.g., oxo, imido) or moderate π-donors (e.g., alkoxo) was critical in the stabilizing and the fine tuning of the reactivity of such metal centers in catalysis. The amido anion NR_2^- has been used extensively as a ligand in early transition metal chemistry[1-3] and is generally considered

(1) Bradley, D. C.; Chisholm, M. H. *Acc. Chem. Res.* **1976**, *9*, 273.
(2) Chisholm, M. H.; Rothwell, I. P. In *Comprehensive Organometallic Chemistry*; Wilkinson, G., Ed.; Pergamon Press: New York, 1982; p 161.

0276-7333/92/2311-2413$03.00/0

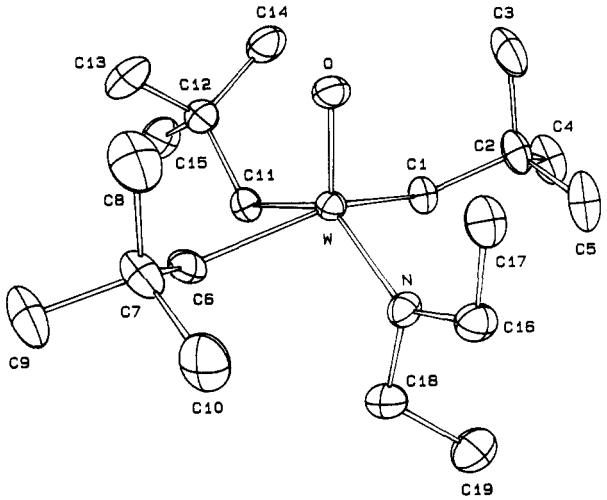

Figure 1. ORTEP plot of one molecule of **2a** showing the numbering scheme used. Ellipsoids are scaled to enclose 50% of the electronic density. Hydrogen atoms are omitted.

to be both a better σ- and π-donor than halide or alkoxide.[1] In our studies on W(VI) complexes with oxo ligands, which originally were synthesized for their potential use as olefin metathesis catalysts,[4] we observed that the simple replacement of a halide or alkoxide by the NR_2 ligand caused a change in the structure of the resultant complex. Further, these amido complexes showed interesting dynamic properties, which were observed by NMR studies. These effects, we believe, can be traced to the stereoelectronic demands of the strongly π-donating amido ligand.

Results and Discussion

(1) Synthesis of Tungsten(VI)–Oxo Complexes with Amido Ligands. The replacement of the halide ligand X by the dialkylamido group NR_2 in the complexes $WO(CH_2Bu^t)_3X$[4] was carried out straightforwardly by the following reaction sequence:

$$WOCl_4 + LiNR_2 \rightarrow WOCl_3(NR_2) + LiCl$$

$$WOCl_3(NR_2) + Mg(CH_2Bu^t)_2 \rightarrow WO(CH_2Bu^t)_2(NR_2)Cl + MgCl_2$$
1

$$WO(CH_2Bu^t)_2(NR_2)Cl + LiCH_2Bu^t \rightarrow WO(CH_2Bu^t)_3(NR_2) + LiCl$$
2

The complexes $WO(CH_2Bu^t)_2(NR_2)Cl$ **1** and $WO(CH_2Bu^t)_3(NR_2)$ **2** were prepared using three different amido ligands, NEt_2 (**a**), NMe_2 (**b**), and $N(CH_2CH_2)_2$ (pyrrolidinate; **c**). The details of their syntheses are given in the Experimental Section. Compound **1a** is colorless, air-sensitive, and subject to decomposition over a few hours in solution at ambient temperature. **1b** is the most unstable and could not be characterized by microanalysis although the ^1H NMR data are consistent with its formulation. The trineopentyl complexes **2a–c** were synthesized in reasonable yield (40–85%). If **2a** is quite stable and gives orange yellow crystals, **2b** is thermally unstable, while **2c** is very sensitive to moisture. Alternatively, these compounds can be obtained directly by reaction of $WO(CH_2Bu^t)_3Cl$ with $LiNR_2$.

Table I. Positional Parameters for 2a[a]

atom	x	y	z	B (Å²)
W	0.09247 (3)	0.13020 (2)	0.15724 (1)	2.059 (9)
O	0.0571 (4)	0.2363 (3)	0.2010 (2)	2.81 (9)
N	0.0553 (5)	0.0006 (4)	0.1948 (3)	2.5 (1)
C1	0.3253 (7)	0.1134 (5)	0.1948 (4)	2.9 (2)
C2	0.4074 (8)	0.1214 (5)	0.2780 (4)	3.5 (2)
C3	0.3902 (8)	0.2281 (7)	0.3067 (4)	5.0 (2)
C4	0.5685 (8)	0.1053 (6)	0.2826 (5)	4.6 (2)
C5	0.3612 (8)	0.0407 (7)	0.3252 (4)	4.8 (2)
C6	−0.0970 (8)	0.1195 (4)	0.0612 (4)	3.0 (2)
C7	−0.2527 (8)	0.1201 (5)	0.0693 (4)	3.6 (2)
C8	−0.2830 (8)	0.2176 (7)	0.1076 (4)	5.0 (2)
C9	−0.3510 (9)	0.1199 (6)	−0.0099 (5)	5.1 (2)
C10	−0.2897 (7)	0.0212 (6)	0.1068 (4)	4.6 (2)
C11	0.1739 (6)	0.1741 (5)	0.0593 (3)	2.7 (1)
C12	0.1863 (7)	0.2922 (5)	0.0443 (4)	3.3 (2)
C13	0.0440 (9)	0.3494 (5)	0.0269 (5)	5.0 (2)
C14	0.2904 (8)	0.3492 (5)	0.1084 (5)	4.2 (2)
C15	0.2478 (8)	0.2993 (6)	−0.0243 (4)	4.7 (2)
C16	0.0042 (8)	−0.0337 (4)	0.2570 (4)	3.1 (1)
C17	−0.0411 (7)	0.0527 (5)	0.3000 (3)	3.2 (2)
C18	0.0785 (7)	−0.0834 (6)	0.1460 (4)	3.8 (2)
C19	0.1800 (9)	−0.1681 (6)	0.1830 (5)	5.0 (2)

[a] Values in parentheses are estimated standards deviations. Anisotropically refined atoms are given in the form of the isotropic equivalent displacement parameters defined as $^4/_3[a^2\beta(1,1) + b^2\beta(2,2) + c^2\beta(3,3) + ab(\cos\gamma)\beta(1,2) + ac(\cos\beta)\beta(1,3) + bc(\cos\alpha) \times \beta(2,3)]$.

Table II. Selected Distances (Å) and Bond Angles (deg) for 2a[a]

W–O	1.667 (4)	W–C6	2.189 (7)
W–N	1.881 (5)	W–C11	2.196 (6)
W–C1	2.184 (6)		
O–W–N	118.8 (2)	C1–W–C11	74.4 (2)
O–W–C1	104.5 (2)	C6–W–C11	76.4 (2)
O–W–C6	101.8 (2)	W–C1–C2	122.6 (5)
O–W–C11	109.4 (2)	W–C6–C7	123.9 (5)
N–W–C1	94.1 (2)	W–C11–C12	116.9 (4)
N–W–C6	92.1 (2)	W–N–C16	135.1 (4)
N–W–C11	131.8 (2)	W–N–C18	111.9 (4)
C1–W–C6	145.8 (3)		

[a] Estimated standard deviations are given in parentheses.

(2) X-ray Structure of $WO(CH_2Bu^t)_3(NEt_2)$. X-ray-quality crystals could only be obtained in the case of **2a**, by slow precipitation of a pentane solution of $WO(CH_2Bu^t)_3(NEt_2)$. The structure is depicted in Figure 1. Final atomic positional parameters for the non-hydrogen atoms are given in Table I. Selected bond distances and bond angles are listed in Table II.

Four equivalent molecules were observed in the monoclinic unit cell. Each tungsten possesses a slightly distorted square pyramidal structure with the oxygen atom on the apical position and C1, C11, C6, and N forming the basal plane. The O–W–N angle of 118.8 (2)° and the O–W–C angles of 101.8 (2)°, 104.5 (2)°, and 109.4 (2)° clearly demonstrate the deformation from the ideal square pyramidal geometry. The tungsten atom is found 0.674 (0) Å out of the basal plane, and the angle between the planes defined by C6, W, C1 and C11, N, O is 89.7 (3)°. Of particular interest is the sum of the angles about the nitrogen atom of the amido ligand (360 (1)°), which indicates that C16, C18, W, and N are coplanar. Furthermore, in the mean plane C16, N, W, O, C11, the maximum deviation is only 0.01 Å for the tungsten atom, which demonstrates that the W=O bond lies parallel to the plane defined by W, N, C16, C18. The notable difference between the angles

(3) (a) Chisholm, M. H.; Cotton, F. A.; Frenz, B. A.; Reichert, W. W.; Shive, L. W.; Stults, B. R. *J. Am. Chem. Soc.* **1976**, *96*, 4469. (b) Chisholm, M. H.; Cotton, F. A.; Extine, M. W.; Stults, B. R. *J. Am. Chem. Soc.* **1976**, *96*, 4477. (c) Akiyama, M.; Chisholm, M. H.; Cotton, F. A.; Extine, M. W.; Murillo, C. A. *Inorg. Chem.* **1977**, *16*, 2407. (d) Chisholm, M. H.; Cotton, F. A.; Extine, M. W.; Millar, M.; Stults, B. R. *Inorg. Chem.* **1976**, *15*, 2244. (e) Chisholm, M. H.; Extine, M. W. *J. Am. Chem. Soc.* **1976**, *98*, 6393.

(4) (a) Fischer, J.; Kress, J.; Osborn, J. A.; Ricard, L.; Wesolek, M. *Polyhedron* **1987**, *6*, 1839. (b) Kress, J.; Wesolek, M.; Le Ny, J. P.; Osborn, J. A. *J. Chem. Soc., Chem. Commun.* **1981**, 1039.

Table III. Activation Energy (in kcal mol^{-1}) for Alkyl Exchange of the NR_2 Group (A) and for Equilibration of Neopentyl Groups (B)

complex	A	B
1a	9	not detectable
2a	18	20
2a·$AlCl_3$	11	13
2b	17	decomposition
2c	16	18
2c·$AlCl_3$	14	13

W–N–C16 of 135.1 (4)° and W–N–C18 of 111.9 (4)° is most likely due to steric repulsion of the nearby neopentyl groups.

Whereas the tungsten–oxygen bond length of 1.667 (4) Å is typical of a double bond[5-8] of this type, the tungsten–nitrogen bond length of 1.881 (5) Å is significantly shorter than previously observed in other W(VI) complexes involving amido ligands. For example, in $W(NMe_2)_6$, the W–N bond is 2.032 (25) Å and theory would predict a bond order of 1.5;[9] however, in $W(NMe_2)_3(O_2CNMe_2)_3$ where a strong π-bond (bond order of 2) would be expected, the W–N bond is 1.922 (7) Å.[10] Therefore, by this criterion, **2a** appears to possess a strong double bond.

(3) NMR Studies. (i) $WO(CH_2Bu^t)_3(NR_2)$ (2a–c). The ^1H NMR spectrum of **2a** is typical of this class of compounds. At ambient temperature, the three neopentyl ligands are not equivalent, in contrast with the observations we previously made on the halide and alkoxo derivatives $WO(CH_2Bu^t)_3X$ (X = Cl, Br, OCH_2Bu^t).[4a] Hence in **2a**, one pair of neopentyl groups shows an AX quartet spectrum for the diastereotopic CH_2Bu^t protons (δ_A 2.68 and δ_X 1.00 ppm, J_{AX} = 15.1 Hz) and a singlet at 1.16 ppm for the two Bu^t groups. The third neopentyl ligand is observed as two singlet resonances at 2.13 (CH_2Bu^t) and 1.54 ppm (CH_2Bu^t). The second important feature of this spectrum is the nonequivalence of the ethyl groups in the NEt_2 ligand even at ambient temperature, with the NCH_2CH_3 quartet resonances at 3.13 and 2.14 ppm, and the NCH_2CH_3 triplets at 1.43 and 0.61 ppm.

When the temperature of compounds **2** in $C_6D_5CD_3$ is raised, the NMR spectra display two significant changes. In the first process A, the resonances of the alkyl groups of the NEt_2 group broaden and eventually coalesce. By measurement of the coalescence temperature T_c ($T_c \approx 390$ (**2a**), 370 (**2b**), and 340 (**2c**) K) and the peak separation of the α-protons of the amido group resonances, and application of the simple Eyring formula,[11] the barrier for equilibration of the ethyl groups can be estimated as $\Delta G^*_{T_c} \approx 18$ (**2a**), 17 (**2b**), and 16 (**2c**) kcal mol^{-1}, respectively (see Table III). For **2c**, at higher temperatures (ca. 370 K), a further process B causes the coalescence of the two different types of neopentyl group resonances. This process is reversible but difficult to measure accurately since slow decomposition takes place; however, it was estimated to occur with a barrier of 18 kcal mol^{-1}. For **2a**, the neopentyl resonances broaden above 400 K but coalescence could not be observed before the onset of extensive decomposition. From the increase in line width of the WCH_2Bu^t resonances at 400 K, a barrier of 20 kcal mol^{-1} was again estimated for neopentyl equilibration in **2a**.

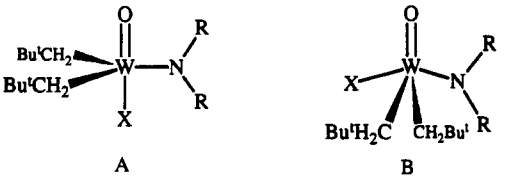

Figure 2. Idealized ground-state structures of $WO(CH_2Bu^t)_2(NR_2)X$, X = Cl, CH_2Bu^t.

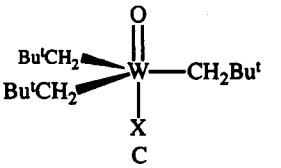

Figure 3. Idealized structure of $WO(CH_2Bu^t)_3X$, X = halogen.

(ii) $WO(CH_2Bu^t)_2(NR_2)Cl$ (1a, 1b). In the ^1H NMR spectrum of **1a** at ambient temperature, the neopentyl ligands show an AB spectrum (δ_A 2.33 ppm, δ_B 1.91 ppm, J_{AB} = 11.6 Hz) for the methylene protons and a singlet resonance for the Bu^t group at 1.38 ppm. The two ethyl groups in the NEt_2 ligand appear equivalent, with a quartet at 3.38 ppm ($N(CH_2CH_3)_2$) and a triplet at 0.69 ppm ($N(CH_2CH_3)_2$, $^3J_{HH}$ = 7 Hz). The ^{13}C NMR spectrum of **1a** confirms these assignments. However when the temperature is lowered, the two ethyl resonances broaden and the two groups become nonequivalent, no other significant changes occurring. From the separation of the NCH_2CH_3 protons (ca. 1 ppm) at low temperature and their coalescence temperature ($T_c \approx 190$ K), a barrier for exchange of the ethyl groups on the NEt_2 ligand can be estimated as $\Delta G^*_{T_c} \approx 9$ kcal mol^{-1}.

At room temperature the NMR spectrum of **1b** shows similar features, but extensive decomposition occurred on raising the temperature.

(4) Structural Considerations. From the ^1H NMR data, two idealized ground-state structures can be proposed for these compounds in solution (Figure 2). Structure A is based on a trigonal bipyramidal stereochemistry about tungsten with the oxo ligand occupying an apical site and the two neopentyl groups in equatorial positions. From the low-temperature NMR results it appears that the NR_2 ligand would then be planar, located in the equatorial site and, importantly, with its plane parallel to the W=O vector.

The alternative structure B is square pyramidal, with the oxo ligand axial and the neopentyl ligands in the basal plane. The NR_2 ligand would also occupy a basal site, again with its plane oriented parallel to the W=O axis. No distinction between A and B can be made on the basis of these NMR data alone, and the difference in energy between the two structures might not be expected to be large (vide infra). However, we note the idealized structure B approximates that found for **2a** in the solid state.

In both possible structures, the NR_2 ligand is oriented so as to place the lone pair on N in the plane orthogonal to the W=O vector, thus avoiding competition with the oxo group in terms of π-donation to the unoccupied orbitals of the formally d^0 W(VI) center.[2,12-16] Thus with

(5) Churchill, M. R.; Missert, J. R.; Youngs, W. J. *Inorg. Chem.* **1981**, *20*, 3388.
(6) Churchill, M. R.; Rheingold, A. L. *Inorg. Chem.* **1982**, *21*, 1357.
(7) Feinstein-Jaffe, I.; Gibson, D.; Lippart, S. J.; Schrock, R. R.; Spool, A. *J. Am. Chem. Soc.* **1984**, *106*, 6305.
(8) Legzdins, P.; Rettig, S. J.; Sanchez, L. *Organometallics* **1985**, *4*, 1470.
(9) Bradley, D. C.; Chisholm, M. H.; Heath, C. E.; Hursthouse, M. B. *Chem. Commun.* **1969**, 1261.
(10) Chisholm, M. H.; Extine, M. *J. Am. Chem. Soc.* **1974**, *96*, 6214.
(11) Günther, H. *NMR Spectroscopy*; J. Wiley: New York, 1980; p 241.
(12) Chisholm, M. H.; Folting, K.; Huffman, J. C.; Rothwell, I. P. *Organometallics* **1982**, *1*, 251.
(13) Chisholm, M. H.; Cotton, F. A.; Extine, M. W.; Millar, M.; Stults, B. R. *Inorg. Chem.* **1977**, *16*, 320.
(14) Hearth, C.; Hursthouse, M. B. *J. Chem. Soc., Chem. Commun.* **1971**, 143.
(15) Versluis, L.; Ziegler, T. *Organometallics* **1990**, *9*, 2985.

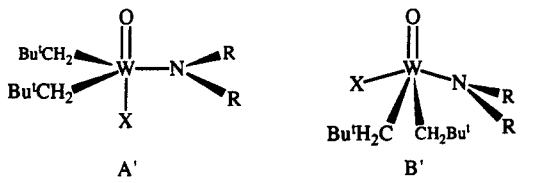

A' B'

Figure 4. Idealized intermediate structures of $WO(CH_2Bu^t)_2(NR_2)X$, X = Cl, CH_2Bu^t.

the oxo ligand (O^{2-}) π-donating into the d_{xz} and d_{yz} orbitals (e'' for TBP and e for SP),[17] the amido ligand will occupy either the equatorial site of a trigonal bipyramid or a basal site in the square pyramid, where its filled p orbital can interact with the vacant d_{xy} orbital (e' for TBP and b_2 for SP). The d_{xy} orbital is of course also further modified by σ-interactions with the neopentyl groups.[17]

It is also interesting to note that structure C (Figure 3) observed for the halide and alkoxide complexes is not found for the analogue containing strongly π-donating amido ligand. Clearly a shift to an equatorial site (in A) or a change in ground-state stereochemistry (as in B), when coupled with the appropriate orientation of the amido ligand, minimizes π-donor competition with the oxo ligand. This influence in fact must dominate over the negative effects resulting from a greater compression of the neopentyl groups about the metal.

(5) Dynamic Behavior. (i) Rotation of the Amido Ligand. The coalescence of the ethyl resonances on raising the temperature can be interpreted as resulting from rotation of the NR_2 group about the W–NR_2 axis[12,13] via an intermediate or transition state in which the plane of the NR_2 group will lie perpendicular to the W=O vector (Figure 4, structure A' or B'). During this process, W–NR_2 σ-bonding will be maintained but the in-plane π-interaction will be lost. Further, in A' (as in B') a repulsive interaction with a filled W–oxo π-interaction will occur, possibly producing some pyramidalization at nitrogen. We note that the value of the rotational barrier is slightly smaller than that typically observed[2,12] (10–15 kcal mol^{-1}) for other amido complexes of W and Mo. Therefore one is initially tempted to attribute the overall barrier observed for this process as resulting from the difference between the $p_\pi(N)$–$d_\pi(W)$ interactions for two orientations of the amido ligand. We will consider this point in terms of two possible structures A and B.

In structure A, if the barrier of this process were to result only from the electronic effects discussed above, it would be difficult to reconcile the much larger values found for **2** (ca. 16–18 kcal mol^{-1}) compared to that of **1a** (ca. 9 kcal mol^{-1}). In structure A, the presence of the bulky neopentyl group in the axial site of **2** (rather than the smaller halide in **1a**) would cause a greater steric interaction with the R groups of the amido ligand in the ground state than in the intermediate A' (Figures 2 and 4) for which the R groups are in the trigonal plane. Hence the barrier might have been expected to be lower in **2**, because of the steric destabilization of the ground state. Furthermore, it is not clear how the electronic effect caused by replacing halide by neopentyl in the axial site in structure A could explain such rotational barrier differences.

However, if structure B obtains, the steric interactions between the amido group and the neopentyl ligand are reduced in the ground state but increased in the intermediate B'. The steric destabilization of the intermediate state would therefore be expected to increase the rotation barrier on passing from **1** to **2**, which indeed is found. In structure B, the overlap between the p_π orbital of the amido nitrogen and the d_{xy} orbital of the tungsten will diminish as the angle O–W–N increases,[17] and since this angle may differ for **1** and **2**, this could also contribute to the difference in the barrier heights. Indeed, we cannot exclude the possibility that **1a** adopts structure A. However, we believe that, overall, the major *difference* in the rotational barriers observed for the compounds **1** and **2** arises predominantly from steric effects, although the p_π–d_π interaction must also provide a significant contribution to the rotational barriers in *both* **1** and **2**.

(ii) Stereochemical Nonrigidity. The energy difference between such square pyramidal and trigonal bipyramidal structures, however, is probably relatively small as illustrated by the high-temperature NMR behavior spectra of **2c** mentioned above, where three neopentyl groups coalesce into a single resonance. The most attractive intermediate for this process would be structure C which, as we have suggested, is at higher energy because of the π-donor competition between oxo and amido ligands. A complex series of Berry pseudorotation operations could be applied to produce such an intermediate, but given the low symmetry of the species involved and the large bonding differences between the ligands, this approach would seem both unreasonably classical and unrealistic.[18] However, whatever the detailed mechanism, the difference in energy between structures B and C cannot exceed this interconversion barrier (ca. 20 kcal mol^{-1}). The passage from B to C will be favored by the steric decompression of the neopentyl groups but disfavored electronically since the amido and oxo ligands are placed in direct π-donor competition. Hence the quasi-cis arrangement of oxo and amido ligands probably is favorable over the trans geometry by much greater than 20 kcal mol^{-1}.

Finally, such intramolecular rearrangements would be expected in pentacoordinate d^0 systems, and it is clear that the stereochemistries of (and the barriers to interconversion in) such molecules may in part be qualitatively related to ligand site preferences as has been long known in phosphorus(V) chemistry.[19]

(6) Further Observations. We have shown[4a] that the complexes $WO(CH_2Bu^t)_3X$ (X = halide, OR) form adducts with Lewis acids such as $AlBr_3$ or $GaCl_3$, where a bond is formed between the Lewis acid and the oxo ligand. We find that the complexes **2** also interact strongly with $AlCl_3$, and we have studied these adducts by NMR to investigate the possible changes in their structure and dynamic properties. When $AlCl_3$ is added to **2a** or **2c** in CD_2Cl_2 solution, all proton resonances are shifted. For example, the methylene protons (CH_2Bu^t) are displaced by 0.5–2 ppm, and the α-protons of the amido ligands (NCH_2R) by 0.2–0.6 ppm. In the infrared spectrum, the ν(W=O) stretching mode is lowered by ca. 30 cm^{-1}; e.g., ν(W=O), for **2a** at 985 cm^{-1}, is found at 955 cm^{-1} in the $AlCl_3$ adduct, indicating binding of $AlCl_3$ to the oxo ligand as found for $WO(CH_2Bu^t)_3X$ (X = halide).[4a]

The two dynamic phenomena previously observed for **2a** and **2c** in the ^1H NMR spectra are equally well observed for the corresponding adducts with $AlCl_3$ but, notably, the coalescence of resonances occurs at much lower temperatures for both processes and the calculated barriers of

(16) Cundari, T. R.; Gordon, M. S. *J. Am. Chem. Soc.* **1991**, *113*, 5231.
(17) Rossi, A. R.; Hoffman, R. *Inorg. Chem.* **1975**, *14*, 375.

(18) (a) Berry, R. S. *J. Chem. Phys.* **1960**, *32*, 933. (b) Altmann, J. A.; Yates, K.; Csizmadia, I. G. *J. Am. Chem. Soc.* **1976**, *98*, 1450. (c) Strich, A. *Inorg. Chem.* **1978**, *17*, 942.
(19) (a) Kwart, H.; King, K. G. *d-Orbitals in the Chemistry of Silicon, Phosphorus and Sulfur*; Springer Verlag: New York, 1977; p 96. (b) Holmes, R. *J. Am. Chem. Soc.* **1975**, *97*, 5379. (c) Hoffmann, R.; Howell, J. M.; Muetterties, E. L. *J. Am. Chem. Soc.* **1972**, *94*, 3048.

activation for the rotation about the W–N bond as well as the stereochemical rearrangement are lower than for **2a** and **2c** (Table III). Binding of the Lewis acid to the oxo ligand will reduce its π-donor ability, and application of the notions discussed above leads to the prediction that both processes should occur at lower energy for the adducts, which is indeed that observed.

Conclusion

We have shown in this work that in a series of tungsten(VI)–oxo complexes the replacement of a halide or alkoxo by an amido ligand can cause a significant change in stereochemistry, which occurs in order to minimize π-donor competition between the two strongly π-donating oxo and amido ligands. Such π-donor effects also manifest themselves in the mechanism and activation barriers of certain intramolecular rearrangement processes observed in these molecules.

Experimental Section

All manipulations were carried out under nitrogen. The solvents were dried and distilled before use. $WOCl_4$ was prepared by reaction of WCl_6 with WO_3[20] and then sublimed. The lithium salts of amines were obtained by the reaction of a secondary amine with *n*-butyllithium. $Mg(CH_2Bu^t)_2$·dioxane was prepared by the classical reaction of the neopentyl bromide with magnesium metal followed by addition of an excess of dioxane. $LiCH_2Bu^t$ was prepared by adding $ClCH_2Bu^t$ on Li metal. NMR spectra were recorded on a Brucker WP 200 instrument; the observation frequencies were 200 and 50 MHz for ^1H and ^{13}C NMR, respectively. The mass spectra were performed on a Finnigan MAT TSQ 70 instrument by chemical ionization (with isobutane as ionizing gas).

Syntheses of $WO(CH_2Bu^t)_2(NR_2)Cl$ (1a, 1b). The synthesis of **1a** was carried out as follows. A 0.27-g (3.4 mmol) sample of $LiNEt_2$ dissolved in 20 mL of diethyl ether was added dropwise to a solution of 1.2 g (3.5 mmol) of $WOCl_4$ in 30 mL of diethyl ether. The solution turned green with concomitant precipitation of LiCl; 0.81 g (3.7 mmol) of $Mg(CH_2Bu^t)_2$·dioxane dissolved in 30 mL of diethyl ether was then slowly added. The solution was stirred for 30 min and filtered, and the solvent was evaporated under vacuum. The brown gum obtained was dissolved in 10 mL of pentane, and the solution cooled to −30 °C; 500 mg of $WO(CH_2Bu^t)_2(NEt_2)Cl$ were obtained as colorless crystals (yield 30%). ^1H NMR (C_6D_6, 200 MHz): δ 3.34 (q, 4 H, $N(CH_2CH_3)$, $^3J_{HH}$ = 7 Hz), 2.28 (d, 2 H, $WCH_aH_bC(CH_3)_3$, $^2J_{H_aH_b}$ = 11.6 Hz), 1.93 (d, 2 H, $WCH_aH_bC(CH_3)_3$), 1.33 (s, 18 H, $WCH_2C(CH_3)_3$), 0.69 (t, 6 H, $N(CH_2CH_3)$). $^{13}C\{^1H\}$ NMR: δ 86.8 ($WCH_2C(CH_3)_3$), 52.06 ($N(CH_2CH_3)$), 34.5 ($WCH_2C(CH_3)_3$), 26.5 ($WCH_2C(CH_3)_3$), 11.1 ($N(CH_2CH_3)$). IR (Nujol) (ν, cm^{-1}); 1210 (m, W–CH_2Bu^t), 970 (s, WO), 280 (m, WCl). Anal. Calcd for $WC_{14}H_{32}NOCl$: C, 37.39; H, 7.17; N, 2.86. Found: C, 37.16; H, 7.06; N, 2.94.

The synthesis of **1b** was carried out in an identical manner. The compound proved to be quite unstable in the solid state, even at ambient temperature, and could only be identified by its ^1H NMR spectrum. ^1H NMR (C_6D_6, 200 MHz): δ 2.92 (s, br, 6 H, $N(CH_3)_2$), 2.00 (s, br, 4 H, $WCH_2C(CH_3)_3$), 1.29 (s, 18 H, $WCH_2C(CH_3)_3$). IR (Nujol) (ν, cm^{-1}): 1220 (w, W–CH_2Bu^t), 980 (s, WO), 300 (m, WCl).

Syntheses of $WO(CH_2Bu^t)_3(NR_2)$ (2a–c). 2a. A 500-mg (1.11 mmol) sample of $WO(CH_2Bu^t)_2(NEt_2)Cl$ was dissolved in 20 mL of pentane, and 120 mg (1.5 mmol) of $LiCH_2Bu^t$ was added as a solid. The solution was stirred for 1 h. A few drops of C_6H_5Cl were then added, and the solvent was evaporated under vacuum. The solid thus obtained was dissolved in 10 mL of pentane, and the solution was filtered and cooled to −30 °C; 450 mg of orange yellow crystals of $WO(CH_2Bu^t)_3(NEt_2)$ were collected (yield 85%). ^1H NMR (C_6D_6, 200 MHz): δ 3.13 (q, 2 H, $N(CH_2CH_3)_{syn\ or\ anti}$, $^3J_{HH}$ = 7 Hz), 2.68 (d, 2 H, $WCH_aH_xC(CH_3)_3$, $^2J_{H_aH_x}$ = 15.1 Hz), 2.14 (q, 2 H, $N(CH_2CH_3)_{anti\ or\ syn}$), 2.13 (s, 2 H, $WCH_2C(CH_3)_3$), $^2J_{WH}$ = 6.4 Hz), 1.54 (s, 9 H, $WCH_2C(CH_3)_3$), 1.43 (t, 3 H, $(CH_2CH_3)_{syn\ or\ anti}$), 1.16 (s, 18 H, $WCH_aH_bC(CH_3)_3$), 1.00 (d, 2 H, $WCH_aH_xC(CH_3)_3$), 0.61 (t, 3 H, $N(CH_2CH_3)_{anti\ or\ syn}$). IR (Nujol) ($\nu$ cm^{-1}): 1210 (m, W–CH_2Bu^t), 985 (s, WO). Anal. Calcd for $WC_{19}H_{43}NO$: C, 47.01; H, 8.93; N, 2.89. Found: C, 46.32; H, 8.53; N, 2.80.

The same general procedure was used for the syntheses of compounds **2b** and **2c**.

2b. $WO(CH_2Bu^t)_3(NMe_2)$ decomposed very rapidly at ambient temperature and could only be characterized by its NMR. ^1H NMR (C_6D_6, 200 MHz): δ 3.46 (s, 3 H, $NCH_{3\ syn\ or\ anti}$), 2.77 (d, 2 H, $WCH_aH_bC(CH_3)_3$, $^2J_{H_aH_b}$ = 15 Hz, $^2J_{WH}$ = 7.5 Hz), 2.11 (s, 2 H, $WCH_2C(CH_3)_3$, $^2J_{WH}$ = 6 Hz), 2.00 (s, 3 H, $NCH_{3\ anti\ or\ syn}$), 1.56 (s, 9 H, $WCH_2C(CH_3)_3$), 1.23 (s, 18 H, $CH_aH_bC(CH_3)_3$), 1.01 (d, 2 H, $WCH_aH_bC(CH_3)_3$).

2c. $WO(CH_2Bu^t)_3(N(CH_2CH_2)_2)$ was synthesized according to the above procedure but using the lithium salt of pyrrolidine. Satisfactory analytical data of **2c** could not be obtained, even after several recrystallizations of different samples, probably because of the extreme sensitivity of **2c** to water. The mass spectra of **2c**, which could not be performed under strictly anaerobic conditions, also showed a major peak at 499 corresponding to $[M + 18]^-$ (expected for **2c** m/z 481). ^1H NMR (C_6D_6, 200 MHz): δ 4.17 (m, 2 H, $N(CH_2^-)_{syn\ or\ anti}$), 2.94 (m, 2 H, $N(CH_2^-)_{anti\ or\ syn}$), 2.80 (d, 2 H, $WCH_aH_bC(CH_3)_3$, $^2J_{H_aH_b}$ = 14 Hz), 2.14 (s, 2 H, $WCH_2C(CH_3)_3$, $^2J_{WH}$ = 6.8 Hz), 1.47 (s, 9 H, $WCH_2C(CH_3)_3$), 1.20 (s, 18 H, $CH_aH_bC(CH_3)_3$) and ~1.20, overlapped by the previous Bu^t group ($N(CH_2CH_2)_2$), 0.90 (d, 2 H, $WCH_aH_bC(CH_3)_3$).

Formation of the Adducts with Lewis Acids ($2a·AlCl_3$ and $2c·AlCl_3$). Freshly sublimated $AlCl_3$ was added as a solid by small portions to a solution of **2a** and **2c** in CD_2Cl_2 until no further shift of the NMR peaks was observed. Such an addition corresponds to ~1 equiv of acid per mole of complex. The solvent was then evaporated to dryness, and the IR spectrum of the solid thus obtained was recorded as a Nujol mull.

$2a·AlCl_3$. ^1H NMR (CD_2Cl_2, 200 MHz, 253 K): δ 4.44 (q, 2 H, $N(CH_2CH_3)_{syn\ or\ anti}$, $^3J_{HH}$ = 7 Hz), 3.44 (s, 2 H, $WCH_2C(CH_3)_3$), 3.40 (d, 2 H, $WCH_aH_xC(CH_3)_3$, $^2J_{H_aH_x}$ = 15 Hz), 2.62 (q, 2 H, $N(CH_2CH_3)_{anti\ or\ syn}$), 1.76 (d, 2 H, $WCH_aH_xC(CH_3)_3$), 1.43 (t, 3 H, $N(CH_2CH_3)_{syn\ or\ anti}$), 1.24 (s, 9 H, $WCH_2C(CH_3)_3$), 1.09 (s, 18 H, $WCH_aH_bC(CH_3)_3$), overlapped by the previous Bu^t group ($N(CH_2CH_3)_{anti\ or\ syn}$). IR (Nujol) ($\nu$ cm^{-1}): 1230 (m, W–CH_2Bu^t), 955 (s, WO).

$2c·AlCl_3$. ^1H NMR (CD_2Cl_2, 200 MHz, 240 K): δ 4.68 (m, 2 H, $N(CH_2^-)_{syn\ or\ anti}$), 3.49 (m, 2 H, $N(CH_2^-)_{anti\ or\ syn}$), 2.49 (d, 2 H,

Table IV. X-ray Experimental Parameters for 2a

formula	$C_{19}H_{43}NOW$
M_r	485.41
color	yellow orange
crystal system	monoclinic
a (Å)	9.632 (2)
b (Å)	12.961 (3)
c (Å)	18.192 (4)
β (deg)	104.62 (2)
V (Å^3)	2197.6
Z	4
d_{calc} (g cm^{-3})	1.467
space group	$P2_1/c$ (No. 14)
radiation	Cu Kα (nickel filtered)
wavelength (Å)	1.5418
F(000)	984
μ (cm^{-1})	98.6
crystal size (mm)	0.20 × 0.16 × 0.12
temperature (°C)	−100
diffractometer	Philips PW1100/16
mode	$\theta/2\theta$ flying step–scan
scan speed (deg^{-1})	0.024
scan width (deg)	1.00 + 0.143 tan θ
step width (deg)	0.05
θ limits (deg)	3/53
octants	$\pm h,+k,+l$
total no. of data collected	2606
no. of data with $I > 3\sigma(I)$	2060
abs min/max	0.92/1.21
R_F	0.0276
R_{wF}	0.0514
ρ	0.08
GOF	1.21

(20) Tillack, J. *Inorg. Synth.* **1973**, *14*, 109.

$WCH_aH_xC(CH_3)_3$, $^2J_{H_aH_x}$ = 15 Hz), 1.74 (s, 2 H, $WCH_2C(CH_3)_3$), 1.04 (s, 9 H, $WCH_2C(CH_3)_3$), 0.86 (s, 18 H, $WCH_aH_bC(CH_3)_3$), 0.67 (d, 2 H, $WCH_aH_xC(CH_3)_3$), overlapped by the previous Bu^t group ($N(CH_2CH_2)_{anti\ and\ syn}$). IR (Nujol) ($\nu$ cm^{-1}): 1230 (m, W-CH_2Bu^t), 960 (s, WO).

X-ray Structure Determination. Suitable orange yellow crystals of **2a** were obtained by slow evaporation of a saturated pentane solution of **2a** and were mounted above a stream of argon. Data were collected on a Philips PW1100/16 diffractometer equipped with a low-temperature device using nickel-filtered Cu Kα radiation (λ = 1.5418 Å). The crystal data and data collection parameters are summarized in Table IV. No significant changes were observed for three standard reflections monitored hourly during the data collection period. The Enraf-Nonius SDP package[21] was used on a Microvax II computer for all calculations, except that a local program was employed for data reduction. The initial step-scan data were converted to intensities by the method of Lehmann and Larson[22] and then corrected for Lorentz polarization and absorption factors, with the latter being computed by the method of Walker and Stuart.[23] The structure was solved using the heavy atom method. The remaining non-hydrogen atoms were located on subsequent difference Fourier maps. Hydrogen atoms were introduced at computed coordinates (C-H = 0.95 Å) with isotropic temperature factors $B(H) = 1 + B_{eqv}(C)$ Å^2. Full least-squares refinements converged to the R factors, shown in Table IV. Final difference maps revealed no significant maxima.

Acknowledgment. We thank the CNRS for financial support.

Registry No. **1a**, 141583-60-0; **1b**, 141583-61-1; **2a**, 141583-62-2; **2a**·$AlCl_3$, 141583-58-6; **2b**, 141583-63-3; **2c**, 141583-64-4; **2c**·$AlCl_3$, 141583-59-7; $Mg(CH_2Bu^t)_2$·(dioxane), 67608-37-1; $ClCH_2Bu^t$, 753-89-9.

Supplementary Material Available: Listings of positional and thermal equivalent parameters for all non-hydrogen atoms (Table S1), temperature factors for anisotropic atoms (Table S2), hydrogen atom positional parameters (Table S3), and bond distances and angles (Table S4) for **2a** (6 pages). Ordering information is given on any current masthead page.

OM9106138

(21) Frentz, B. A. In *Computing in Crystallography*; Schenk, H., Olthof-Hazekamp, R., van Koningaveld, H., Bassi, C. G., Eds.; Delft University Press: Delft, The Netherlands, 1978; p 64.
(22) Lehmann, M. S.; Lansen, F. K. *Acta Crystallogr.* 1974, *A30*, 580.
(23) Walker, N.; Stuart, D. *Acta Crystallogr.* 1983, *A39*, 158.

Kinetics and Mechanism of Substitution Reactions of the 17-Electron Complexes $\{\eta^5\text{-}C_5R_5Cr(CO)_3\}$ (R = H, Me) with Tertiary Phosphines

W. Carl Watkins, Kristine Hensel, Suzanne Fortier,* Donal H. Macartney,* and Michael C. Baird*

Department of Chemistry, Queen's University, Kingston, Ontario, Canada K7L 3N6

Stephan J. McLain

Central Research and Development Department, Experimental Station, E. I. du Pont de Nemours & Company, Wilmington, Delaware 19898

Received December 20, 1991

A kinetics investigation of the substitution reactions of the compounds $\{\eta^5\text{-}C_5R_5Cr(CO)_3\}$ (R = H, Me) with tertiary phosphines L to form the substituted radicals $\{\eta^5\text{-}C_5R_5Cr(CO)_2L\}$ is described. The nature of the observed rate laws, the activation parameters, and the steric effects suggest that an associative mechanism pertains, although an interchange-associative process may apply in the case of the back-reaction of the bulky $\{\eta^5\text{-}C_5Me_5Cr(CO)_2(PMe_2Ph)\}$ with CO. The substitution reactions are accompanied by disproportionation processes to form $[\eta^5\text{-}C_5H_5Cr(CO)_2L_2][\eta^5\text{-}C_5H_5Cr(CO)_3]$ (via the monosubstituted cationic complexes $[\eta^5\text{-}C_5H_5Cr(CO)_3L][\eta^5\text{-}C_5H_5Cr(CO)_3]$) and/or by formation of the substituted hydrides $\eta^5\text{-}C_5R_5Cr(CO)_2LH$, depending on the reaction conditions. The X-ray crystal structure of the substituted hydride $\eta^5\text{-}C_5R_5Cr(CO)_2(CDPP)H$ (CDPP = cyclohexyldiphenylphosphine) is described; the compound assumes a cisoid geometry.

Organotransition-metal chemistry has long been dominated by compounds containing closed-shell configurations and obeying the 18-electron rule,[1] but recent years have seen the development of a very extensive chemistry of 17-electron complexes.[2] The latter class of paramagnetic, metal-centered radicals is now known to play important roles as reactive intermediates in many types of reactions, but several examples have proven sufficiently persistent that they have been isolated and characterized both spectroscopically and crystallographically.[2] Of particular relevance here, and in contrast to the chemistry of most 18-electron complexes,[1] which generally undergo ligand substitution reactions via dissociative pathways,[3] several 17-electron compounds have been found to undergo substitution reactions that proceed via associative processes.[4]

(1) Collman, J. P.; Hegedus, L. S.; Norton, J. R.; Finke, R. G. *Principles and Applications of Organotransition Metal Chemistry*; University Science Books: Mill Valley, California, 1987.
(2) (a) Baird, M. C. *Chem. Rev.* 1988, *88*, 1217. (b) Trogler, W. C., Ed. *Organometallic Radical Process*; Elsevier: Amsterdam, 1990.
(3) (a) See: ref 1, chapter 4. (b) Howell, J. A. S.; Burkinshaw, P. M. *Chem. Rev.* 1983, *83*, 557.
(4) (a) Trogler, W. C. In *Organometallic Radical Process*; Trogler, W. C., Ed.; Elsevier: Amsterdam, 1990; p 306 and references therein. (b) Tyler, D. R. In *Organometallic Radical Process*; Trogler, W. C., Ed.; Elsevier: Amsterdam, 1990; p 338 and references therein. (c) Stiegman, A. E.; Tyler, D. R. *Comments Inorg. Chem.* 1986, *5*, 215. (d) Shi, Q.-Z.; Richmond, T. G.; Trogler, W. C.; Basolo, F. *J. Am. Chem. Soc.* 1984, *106*, 71.

0276-7333/92/2311-2418$03.00/0